Nuclear Instruments and Methods in Physics Research A 366 (1995) 76-78

NUCLEAR INSTRUMENTS & METHODS IN PHYSICS RESEARCH Section A

ELSEVIER

# First experimental results from a microdot gas avalanche detector integrated onto a silicon wafer

S.F. Biagi *, J. Bordas, D. Duxbury, E. Gabathuler, T.J. Jones, S. Kiourkos

*Department of Physics, University of Liverpool, P.O. Box 147, Liverpool L69 3BX, UK*

Received 2 May 1995; revised form received 26 June 1995

**Abstract**

First results on the voltage dependence of the gas gain of a microdot detector are presented. No variation of the gas gain with rate is observed up to a measured maximum rate of $4 \times 10^3$ X-rays/mm$^2$/s. Some possible applications of this detector are discussed.

## 1. Introduction

Experiments at future high intensity colliding beam machines and at high intensity synchrotron radiation facilities require a detector which has an intrinsic high rate capability, good imaging or spatial resolution and excellent stability in a high radiation environment. Microstrip gas avalanche (MSGC) and microgap detectors possess some of these properties except for the imaging capability.

Microdot gas avalanche detectors, as proposed in a previous publication, should possess all the above properties [1]. The structure is inherently pixel-like and is probably most suited to experiments operating in a very high rate environment.

## 2. Chamber geometry

Microdot detectors comprising 16 different types of cell geometry have been constructed on 4 in. diameter silicon wafers using a standard MOS process line [2]. Fig. 1 shows a schematic of one of the cell geometry/pixel structures whose properties have been measured and are reported below. The figure shows a view of the cell from above and in cross section through the substrate. For ease of readout the structure has been implemented using a back plane bus to read out the hexagonal close packed pixel structures. The back plane consists of strings of pixels on a 200 $\mu$m pitch readout bus, as shown by the "metal 1" layer indicated in Fig. 1. The bus readout system can be viewed as a method that reduces costs and increases yield when compared with the implementation of a full pixel readout system. The extension of this design to a full pixel system involves the addition of the microdot structure on a pre-existing pixel-amplifier structure and poses no great technical difficulty.

The processing steps used in the manufacture of the microdot chamber are:

(1) first oxide deposit to 2 $\mu$m depth,
(2) metal 1 deposition and etch,
(3) second oxide deposition to 1.8 $\mu$m depth,
(4) ion implantation,
(5) oxide via etch,
(6) metal 2 deposition and etch.

Note that the feature-sizes used are large in comparison with those encountered in state-of-the-art integrated circuit fabrication and hence a pixel yield of > 99% over the full wafer is obtained.

For the measurements reported below, the signal from a group of $\sim$ 3500 pixels, arranged in 14 pixel-strings of 60 mm length, was input to an ORTEC 142AH preamplifier. No passivation was applied to any region of the detector.

## 3. Results

In a previous paper [1], the properties of a microdot chamber were investigated through numerical simulation. The results showed that the microdot could be operated in two different modes characterised by the electric field strength in the drift region. If the drift field is high, a non-linear energy response is obtained at large gas gain. Conversely, at low drift fields the detector response is proportional to the energy and independent of the gas gain. The results presented here are for the latter mode. For all measurements the drift voltage, $V_d$, was set $\sim$ 20 V above the cathode voltage, $V_c$. The gas gap used was 3 mm and the results were obtained using an $^{55}$Fe X-ray source.

The chamber gases used were different mixtures of argon and dimethyl ether (DME), mixed using a standard gas rack.

* Corresponding author.


*SSDI* 0168-9002(95)00687-7

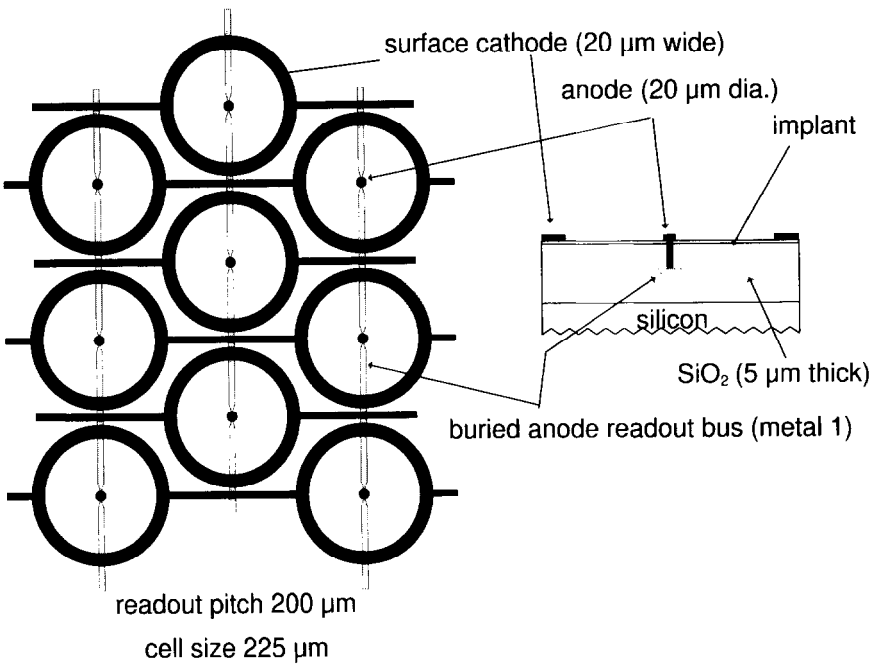


Fig. 1. Mask layout of microdot structure.

This was calibrated by the volume displacement method giving a mixture ratio accuracy of ~ 1%. The absolute gain was determined by two methods. (1) The calibration of the electronics chain, performed by injecting a pulse of known amplitude into the pre-amplifier. (2) Measurement of the chamber current, performed using a Keithley 237 source measure unit, and the X-ray rate.

Fig. 2 shows the measured gas gain as a function of the cathode voltage for different Ar/DME gas mixtures. The maximum operating voltage in each gas mixture was defined by the onset of a current limit trip of 20 nA set on the Keithley 237 source measure unit supplying the surface cathodes.

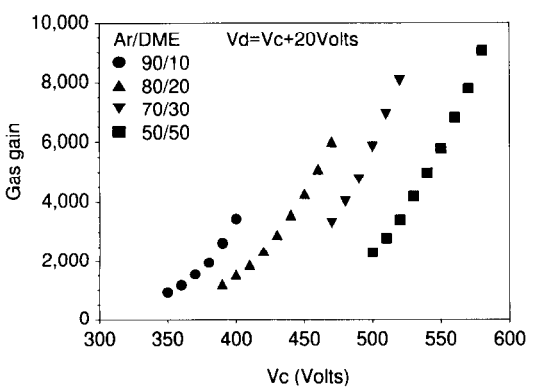


Fig. 2. Gas gain as a function of cathode voltage for different Ar/DME mixtures.

This limit, derived from experience with MSGCs, marks the onset of micro discharges between the anode and surface cathode. These results may be compared to those obtained using standard MSGCs on semi-conducting glass [3]. In general, the results show a similar gas gain dependence with gas mixture, but the microdot chamber operates typically 120 V lower than the MSGC, and with a much reduced drift field, for the same gas gain. Moreover, the maximum "sustainable" (i.e. without electrode erosion) gas gain for the MSGCs in Ref. [3] is ~ 7000 compared with ~ 9000 for the microdot.

The gas gain is limited by the creation of a small high field region between the buried anode readout bus and the surface cathode at the point of intersection. Results from simulation show that there is insufficient shielding current at this point. A small modification to the cell geometry has been devised which should eliminate the problem and allow higher gas gains to be achieved in the low drift field mode of operation.

The gain dependence with rate was measured using a 10 mCi $^{55}Fe$ source placed directly on the detector giving a rate of $4 \times 10^3$ X-rays/mm$^2$/s. At a gas gain of 2000 in Ar/DME (80:20) no change in gain was observed. This corresponds to a minimum ionising charged particle flux of $3 \times 10^4$ mm$^2$/s. This shows that the positive ions from the avalanche are being cleared from the surface by conduction currents in the implanted oxide. Note that in the low drift-field mode of operation, > 90% of the positive ion current is collected on the surface cathodes unlike the MSGC for which ~ 50% is collected.

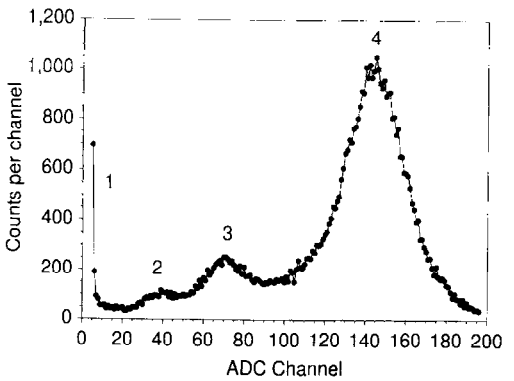


Fig. 3. $^{55}$Fe pulse height spectrum at a gas gain of 2000 in Ar/DME (80:20).

Fig. 3 shows a $^{55}$Fe spectrum at a gas gain of $\sim$ 2000 in Ar/DME (80:20). Four distinct features can be identified: (i) carbon fluorescence X-rays and electronic noise; (ii) aluminium and silicon fluorescence X-rays; (iii) an $^{55}$Fe escape peak; and (iv) an $^{55}$Fe main peak. Previously the noise in thin-oxide MSGCs has been too high to clearly observe the aluminium and silicon peaks which can clearly be seen with microdot detectors.

## 4. Possible applications

The microdot detectors described above have bussed anode readout only. However, by interconnecting the cells in different ways it is possible to develop structures of two types, giving 2D and pixel detectors.

### *4.1. 2D detectors*

Both the anode and surface cathode can be read out in different directions allowing the position of a particle to be determined by two coordinates. These coordinates are most easily defined with stereo angles of 30° multiples, e.g. 30, 60, 90, due to the geometric properties of the hexagonal close packing. More complex interconnections are possible, e.g. fan geometry, but require more effort in mask design. The full avalanche charge is induced on the surface cathodes giving a uni-polar pulse. In contrast, the 2D MSGC designs using a segmented back plane [4] suffer from bi-polar pulses of reduced amplitude compared with the anode pulse. This may make the 2D MSGC design unsuitable for tracking MIPs, although good results have been obtained for X-ray imaging.

### *4.2. Pixel detectors*

Recent progress in the electronics for silicon diode pixel detectors has resulted in the development of pixel amplifier arrays [5]. Since microdot detectors have been fabricated using standard MOS processing it is possible to consider the development of an integrated microdot/amplifier structure. The microdot pattern becomes part of the pixel amplifier array, eliminating the need for bump bonding, as required in silicon diode pixel detectors. Given a typical pixel amplifier noise of 300 electrons and a gas gain of 3000, a signal-to-noise ratio of 10:1 may be obtained for single-photon imaging in applications with a CsI-coated photo-sensitive drift cathode. The reduced ion current flow to the drift cathode should allow the photo-sensitive drift cathode to survive without ageing problems caused by positive ion bombardment.

Simulation of single-photon imaging shows that by using a reduced gas pressure the avalanche can be allowed to develop in the drift space. Hence the charge is shared between many pixels and charge centroid weighting can give a positional accuracy of $\sim$ 10–20 $\mu$m compared to a pixel size of $\sqrt{12}$. An additional advantage of low pressure operation is the possibility of grouping together several cells into one pixel amplifier. The hexagonal tiling naturally allows groups of 4, 7, 9 or more cells to be grouped together with a proportional reduction in the number of readout channels whilst maintaining the same resolution due to the spread of charge between cells.

## 5. Conclusions

The first experimental observation of the gas gain and rate behaviour of a microdot gas avalanche detector has been reported. The detectors behave as predicted by simulation. These results show that the microdot detector is, without further development, suitable for X-ray imaging and particle tracking using the 2D capability. Further development could lead to high resolution, single-photon imaging detectors when coupled to pixel amplifier arrays. Such a system may also be of interest in future high rate experiments.

## Acknowledgements

We would like to thank Dr. Robin Thompson and Evelyn Agnew of HMEL for their invaluable contribution to the manufacture of the microdot detector wafers.

## References

[1] S.F. Biagi and T.J. Jones to be published in Nucl. Instr. and Meth.
[2] Hughes Microelectronics Europa Limited (HMEL), Glenrothes, Scotland.
[3] L. Alunni, R. Bouclier, G. Fara, C. Garabatos, G. Manzin, G. Million, L. Ropelewski, F. Sauli, L. Shekhtman, E. Daubie, O. Pingot, Y.N. Pestov, L. Busso and S. Costa, Nucl. Instr. and Meth. A 348 (1994) 344.
[4] F. Angelini, R. Bellazzini, A. Brez, T. Lomtadze, M.M. Massai, R. Raffo, G. Spandre and M. Spezziga, Nucl. Instr. and Meth. A 336 (1993) 106.
[5] M. Raymond, G. Hall, M. Lovell, P. Sharp, C. Lewin and P. Seller, Nucl. Instr. and Meth. A 348 (1994) 673.